Effects of Variance in Mini Amplitude on Stimulus-Evoked Release: A Comparison of Two Models

Matthew Frerking and Martin Wilson
Section of Neurobiology, Physiology and Behavior, Division of Biological Sciences, University of California, Davis, California 95616 USA

ABSTRACT The strength of synaptic connections between two neurons is characterized by the number of release sites (N) on the presynaptic cell, the probability (p) of transmitter release at those sites in response to a stimulus, and the average size (A) of the postsynaptic response from each site. Quantal analysis can determine N, p, and A, but the large variance in the amplitudes of minis at central synapses is predicted to obscure quantal peaks and render quantal analysis unusable. Recently it has been suggested that the variance in mini amplitude is generated by differences between release sites, rather than by quantum-to-quantum fluctuations at identical sites, and that this form of variance in mini amplitude reduces the amount of variance expected in quantal peaks. Using simulations, we examine the possibility of resolving quantal peaks assuming either form of variance in mini amplitude. We find that individual quantal peaks are resolvable in neither case, provided that the uniquantal distribution is similar to the mini distribution. Because this lack of resolution compromises the utility of quantal analysis, we develop a general description that can solve N and p, given the statistical parameters of the mini distribution and the evoked distribution. We find that this description is relatively insensitive to the source of variance in mini amplitude.

INTRODUCTION

When the probability of transmitter release from a motor neuron is low, postsynaptic responses in a muscle fiber vary randomly between integer multiples of the "spontaneous" miniature response. Briefly stated, this is the evidence for the quantal theory of synaptic transmission as developed by Katz and others (Fatt and Katz, 1952; del Castillo and Katz, 1954; Boyd and Martin, 1956a,b; Liley, 1956). This theory identifies three parameters determining the size of a stimulus-evoked response: the average size of the quantal unit (A), the number of sites (N) that can release a quantum, and the probability of release at each site (p) in response to stimulation. Determining the values of these parameters in the central nervous system, especially in the mammalian CNS, has proved to be very difficult, partly because of technical problems (reviewed in Jack et al., 1994; Stricker et al., 1994), but also because of complications not apparent at the neuromuscular junction.

Quantal analysis is the most widely used method for determining N, p, and A. Quantal analysis treats the probability density function (PDF) of stimulus-evoked amplitudes of either current or voltage as a multimodal distribution in which each mode represents a different number of quanta released (the quantal number). The distributions associated with each quantal number (the quantal peaks) are assumed to add together independently to produce the PDF. Determining A by quantal analysis, assuming a normal distribution of uniquantal responses, requires only that the modes of each quantal peak be resolvable. Moreover, the value of A can be independently verified by examining spontaneous events (minis) which, by analogy with the neuromuscular junction, are thought to be uniquantal. Determining N and p, however, requires that the number of stimulus-evoked events in each quantal peak be accurately determined.

It has commonly been observed that in central neurons, minis, the postsynaptic responses to the release of single quanta, are highly variable in amplitude (Bekkers and Stevens, 1989; Edwards et al., 1990; Ropert et al., 1990; Malgaroli and Tsien, 1992; Manabe et al., 1992; Silver et al., 1992; Otis and Mody, 1992; Rekling, 1993; Ulrich and Lüscher, 1993; Wyllie et al., 1994; De Koninck and Mody, 1994; Tang et al., 1994; Jonas et al., 1993; Tong and Jahr, 1994; Frerking et al., 1995). If this variance reflects trial-to-trial fluctuations at identical release sites, as is thought to be the case at the neuromuscular junction, then the variance of responses corresponding to a certain number of quanta released will be the variance of responses to a single quantum, multiplied by the quantal number. It follows from this that quantal peaks ought to be difficult to resolve at central synapses.

Surprisingly, it is believed that quantal peaks can be seen in central neurons (Jack et al., 1981; Redman and Walmsley, 1983; Walmsley et al., 1988; Edwards et al., 1990; Larkman et al., 1991; Kullmann and Nicoll, 1992; Larkman et al., 1992; Jonas et al., 1993; Kullmann, 1993; reviewed in Jack et al., 1994; reviewed in Stricker et al., 1994), and even more surprisingly, it has been suggested that the variance of individual quantal peaks does not increase linearly with increasing quantal number (but see Kullmann, 1993; Bekkers and Stevens, 1995). It was first suggested that the quantal peaks have only that variance attributable to noise (Jack et al., 1981; Redman and Walmsley, 1983; Walmsley et al., 1988; Stricker et al., 1994). Other experiments suggested that the variance of each quantal peak is largely

Received for publication 22 September 1995 and in final form 7 February 1996.

Address reprint requests to Dr. Martin Wilson, Section of Neurobiology, Physiology and Behavior, Division of Biological Sciences, University of California, Davis, CA 95616. Tel.: 916-752-7250; Fax: 916-752-1449; E-mail: mcwilson@ucdavis.edu.

0006-3495/96/05/2078/14 $2.00

independent of quantal number (Edwards et al., 1990; Larkman et al., 1991). Recently it was suggested that the variance of each quantal peak is nonlinearly dependent on the quantal number (Jack et al., 1994) in such a way that the variance of a quantal peak decreases as the quantal number increases for large quantal numbers, making peaks at large quantal numbers easier to resolve than those at intermediate quantal numbers (Jack et al., 1994). These observations led to a model in which the observed variance in mini amplitude is due, not to trial-to-trial fluctuations, but rather to differences in mini amplitude between release sites at different locations (Edwards et al., 1990; Jonas et al., 1993; reviewed in Jack et al., 1994, and von Kitzing et al., 1994).

This model has a necessary corollary and two important consequences for synaptic biology. Because the variance in mini amplitude would be generated by differences between sites, the mini amplitude at a single site would be invariant, or nearly so. To reconcile this prediction with variance due to the stochastic nature of postsynaptic channel opening and closing, a necessary corollary of this model is that postsynaptic receptors are saturated during neurotransmitter release (Edwards et al., 1990; but see Faber et al., 1992). A consequence of this is that any apparent change in quantal content during synaptic plasticity will necessarily be due to postsynaptic rather than presynaptic modifications. A second consequence of this model is that quantal analysis becomes complicated by the inclusion of the different size classes of minis representing the amplitudes at different release sites. The results obtained from quantal analysis, therefore, will depend on an assumption about whether mini amplitude variance occurs between sites or within them.

The source of variance in mini amplitude is, in most systems, currently unknown. In principle, this issue could be easily resolved by examining the mini amplitudes at a single release site, and this approach has been attempted several times (Bekkers et al., 1990; Bekkers and Stevens, 1995; Liu and Tsien, 1995; Murphy et al., 1995). Results from these experiments uniformly suggest that a large variance in mini amplitude exists within single release sites, supporting the orthodox interpretation of quantal analysis. A criticism of these studies, however, is that it is difficult to know with certainty that only a single release site is under observation (Korn and Faber, 1991; Jack et al., 1994). Less direct methods of determining the source of variance in mini amplitude have been hampered by the fact that there is little theoretical basis for a comparison of the two models for variance in mini amplitude.

To perform simulations establishing a basis for comparison, we have used quantitative data drawn from our previously published work on cultured retinal amacrine cells. The mini distribution at cultured amacrine cell synapses, like that of many other central neurons in slices and in culture, shows a large variance and positive skew (Frerking et al., 1995). The coefficient of variation (CV; standard deviation over mean) of this mini distribution averages ~60% (Frerking et al., 1995), around three times the CV of the mini distribution at the neuromuscular junction (about 20%; Boyd and Martin, 1956a). Assuming the mini distribution from amacrine cells equals the distribution in response to uniquantal release of transmitter, we have modeled the mini distribution as being due to variance either within or between individual release sites to get predictions testable by quantal analysis for each model. First, we examine how the skew of the mini distribution is expected to affect the properties of quantal peaks, and how these expected effects depend on the model for variance in mini amplitude. Second, we examine how quantal peak resolution depends on the model for variance in mini amplitude; in particular, we examine the idea that variance in mini amplitude due to differences between sites could, by itself, reduce the variance during stimulus-evoked release enough to allow quantal peak resolution where this would be impossible with variance in mini amplitude intrinsic to each site. We find that quantal peak resolution is not expected, regardless of which model for variance in mini amplitude applies if the uniquantal distribution is similar to the mini distribution.

Because our predicted inability to resolve quantal peaks makes it unlikely that traditional quantal analysis will be of any use in analyzing actual experimental data, we take a novel alternative approach to solving for N and p. We derive here a general statistical description for stimulus-evoked synaptic currents with either or both forms of variance in mini amplitude present, and consider the limiting cases where either form of variance exclusively accounts for variance in the mini distribution. We find that this method is relatively insensitive to which source of variance in mini amplitude applies. We further find that the relationship between evoked variance and the $N \cdot p$ product is fit by a single parabola, regardless of which model for variance in mini amplitude applies. This implies that changes in N, p, and A could be readily resolved using this technique, regardless of the source of variance in mini amplitude.

METHODS

Calculations were performed using Sigma Plot (Jandel Scientific Software, San Rafael, CA). The Sigma Plot transform language was used for Monte Carlo simulations, convolutions, combinatorial statistics, and construction of equations to fit the mini distribution. The results of simulations were analyzed by eye. Results of Monte Carlo simulations were compared to theoretical distributions by the Kolmogorov-Smirnov test. Unless otherwise stated, $\alpha = 0.05$. Results are presented as mean ± standard deviation.

Our assay for resolving quantal peaks is deliberately qualitative and subjective; we have examined the simulations by eye to see if quantal peaks are resolvable. Our rationale for this is as follows. Complex fitting procedures such as maximum likelihood analysis are excellent at pulling peaks out of noisy data, and could conceivably find peaks with better resolution than analysis by eye, but they suffer from three major failings. First, they are model dependent. The fit is only an accurate description of the data if the model is appropriate, and there is no way a priori to tell if this is the case; indeed, the argument over whether variance in mini amplitude occurs within sites or between them is important because these two models predict different results and the data generally cannot convincingly point to one model over the other. Second, they tend to overfit data

unless efforts are taken to deliberately smooth the data, reducing the resolving power of the fit (Kullmann, 1992). Third, although they provide the best solution for a particular model, they do not rule out different solutions for the same model, nor do they address the likelihood of the unlimited number of alternative models.

RESULTS

Effects of variance in mini amplitude on quantal peaks: an overview

Experiments using quantal analysis typically involve collection of hundreds of responses to stimulation, construction of histograms of synaptic current or voltage amplitude from the data records, and fitting of histograms to a series of gaussian distributions. Each gaussian is generally thought to represent a single quantal peak. When not constrained by a particular model, the mean, variance, and size of each quantal peak are estimated by the corresponding parameters of the fitted gaussians and are used to provide information about A, p, N, and the amount of "quantal variance," i.e., the amount of variance that is linearly dependent on quantal number. The conclusions obtained by this technique depend entirely on the ability to resolve the parameters of quantal peaks. As we will show, the skewed mini distribution that we have simulated cannot generate resolvable quantal peaks, regardless of which model for mini amplitude applies. For completeness, however, we will consider the expected effects of mini-variance on the parameters of individual quantal peaks with the caveat that we are skeptical that this information could be recovered from actual experimental data.

Because the exact effects of mini amplitude variance on responses due to a single quantal number depend quantitatively on the mathematical description of the mini amplitude distribution, we will explore these effects in a mainly qualitative way so as to emphasize the general conclusions rather than those dependent on the exact form of the distribution. The mini distribution in amacrine cells, like that seen in other central neurons (Bekkers and Stevens, 1989; Edwards et al., 1990; Ropert et al., 1990; Malgaroli and Tsien, 1992; Manabe et al., 1992; Silver et al., 1992; Otis and Mody, 1992; Rekling, 1993; Ulrich and Lüscher, 1993; Wyllie et al., 1994; De Koninck and Mody, 1994; Tang et al., 1994; Tong and Jahr, 1994; Jonas et al., 1993), is positively skewed (Frerking et al., 1995). We have previously shown that for amacrine cells this distribution has a shape statistically indistinguishable from a sixth-power gaussian (Frerking et al., 1995), and we will use the sixth-power gaussian as a tentative mathematical description of the mini distribution. We have kept the form of this distribution but reduced the CV to 50%, a procedure that would make quantal peaks easier to resolve than we would anticipate under average conditions and therefore increases the generality of our conclusions.

We start with the case where all variance in mini amplitude is intrinsic to each release site. Recent experiments using quantal analysis have emphasized the removal of baseline noise from histograms through deconvolution (Jack et al., 1981; Korn et al., 1981, 1982; Redman and Walmsley, 1983; Walmsley et al., 1988; Larkmann et al., 1991; Kullmann and Nicoll, 1992; Stricker et al., 1994); however, noise represents a small fraction of variance in mini amplitude (Frerking et al., 1995), and we will ignore it except where it would make a discrete distribution continuous.

Effects of variance intrinsic to single release sites

If all variance in mini amplitude is an intrinsic property of each release site, all release sites have identical mean mini-amplitudes, and the entire skewed mini distribution observed is generated by each release site during multiquantal release. Sources of variance intrinsic to each site include stochastic channel properties and trial-to-trial variations in neurotransmitter concentration. The distribution of responses due to a single quantal number can be generated by convolving the mini distribution against itself a number of times equal to the quantal number minus one. Fig. 1 *A* shows the result of this convolution for multiquantal responses ranging in quantal number from 2 to 8, as well as the mini distribution used in the convolution. The distribution of stimulus-evoked current amplitudes expected during measurements of a simple binomial release process, in which the quantal number varies from trial to trial, is shown in Fig. 1 *B*, where the number of release sites, N, is 8 and the probability of release, p, is 0.5 at each site. It is readily apparent from Fig. 1 *B* that the underlying quantal nature of release under these conditions is completely obscured.

As predicted, the mean (Fig. 1 *C*, *circles*) and variance (Fig. 1 *D*, *circles*) associated with each quantal peak increase linearly and in uniform increments with an increase in quantal number; however, the skew of the mini distribution produces two unanticipated effects. Because the mean is not equal to the mode in a skewed distribution, the difference in amplitude between the mode of the first peak and zero current will be smaller than the difference in amplitude between successive modes. The skewed mini distribution also causes each quantal peak to have a different shape (Fig. 1 *A*); the skew associated with each quantal peak decreases as the quantal number increases (Fig. 1 *D*, *squares*), as predicted by the central limit theorem (Lapin, 1975). These two effects combine to make the modes of the quantal peaks nonquantally separated (Fig. 1 *C*, *squares*).

In summary, a skewed mini distribution with variance that is intrinsic to each release site causes multiquantal release that has linear increases in the mean and variance with increasing quantal number. However, the modes are not quantally separated, and each quantal peak has a different shape due to the skew of the mini distribution. Furthermore, the large measured CV of the mini distribution (Frerking et al., 1995) predicts that individual quantal peaks will be completely unresolvable.

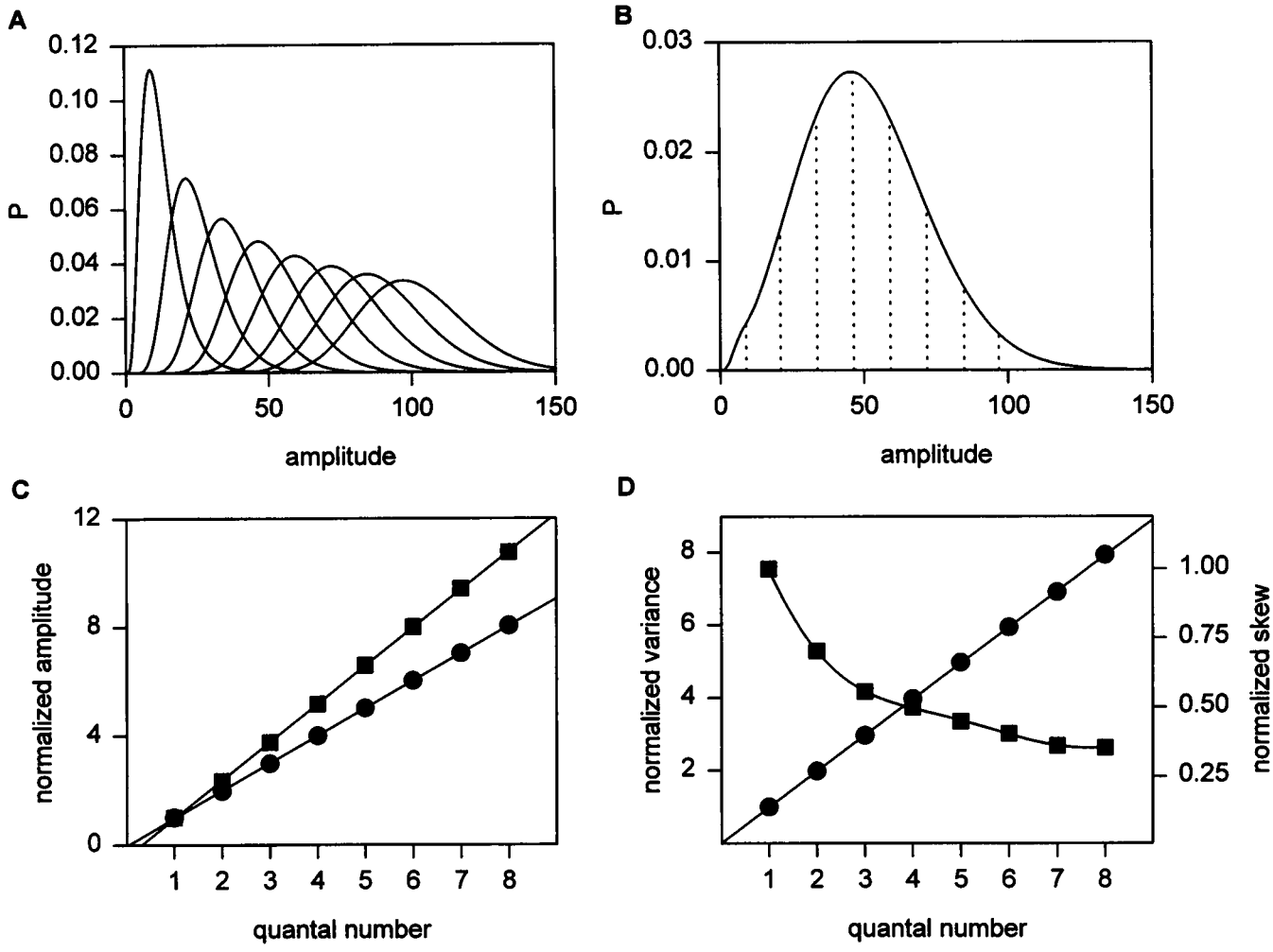

FIGURE 1 The effects of variance in mini amplitude that is intrinsic to single release sites. (*A*) The individual quantal peaks, increasing in quantal number from left (1) to right (8), are shown. The mini distribution (the curve with quantal number, q, equal to 1) is modeled as a sixth-power gaussian, consistent with observations in cultured amacrine cells (Frerking et al., 1995). The larger quantal numbers were generated by numerically convolving the mini distribution against itself $q - 1$ times. (*B*) The distribution of synaptic current amplitudes expected when the mini distribution in *A* is identically sampled at eight different release sites, each with a probability of release of 0.5. Trials in which all sites fail to release an event compose less than 1% of the total and have been excluded. Drop lines indicate mode amplitudes at each quantal number and therefore indicate the location of the part of each quantal peak that will be easiest to resolve. (*C*) The mean (●) and mode (■) of each quantal peak are normalized with respect to their values for the first quantal peak. For a parameter to be quantal, its normalized value must increase linearly with quantal number and the slope of this line must be 1; only the mean passes both of these criteria. (*D*) The variance of each quantal peak (●) increases linearly as quantal number increases, whereas the skew of each quantal peak (■) decreases as quantal number increases.

Effects of variance between individual release sites

If all variance in mini amplitude is due to differences between sites, the distribution of mini amplitude per release site is sampled without replacement during multiquantal release. This is because, unlike the previous case, each site has its own unique amplitude and can only contribute a single mini of that amplitude to simultaneous release from multiple sites. Variance between sites might be generated by differences in the amount of cable filtering at proximal and distal release sites, or by differences in receptor number from one site to the next. Although some models have proposed that the number of receptors at each site is itself quantized (Edwards et al., 1990), we consider the more general case where the mini amplitude at each site is unconstrained.

A mini distribution with a mean, variance, and number of release sites similar to the distribution in Fig. 1 *A* is shown in Fig. 2 A_1, but this distribution is constructed entirely by differences between sites. Because noise would necessarily smear these discrete amplitude peaks, allowing the individual discrete amplitudes at each site to overlap and summate, we show the distribution both before (drop lines) and after (continuous distribution) convolution, with gaussian noise

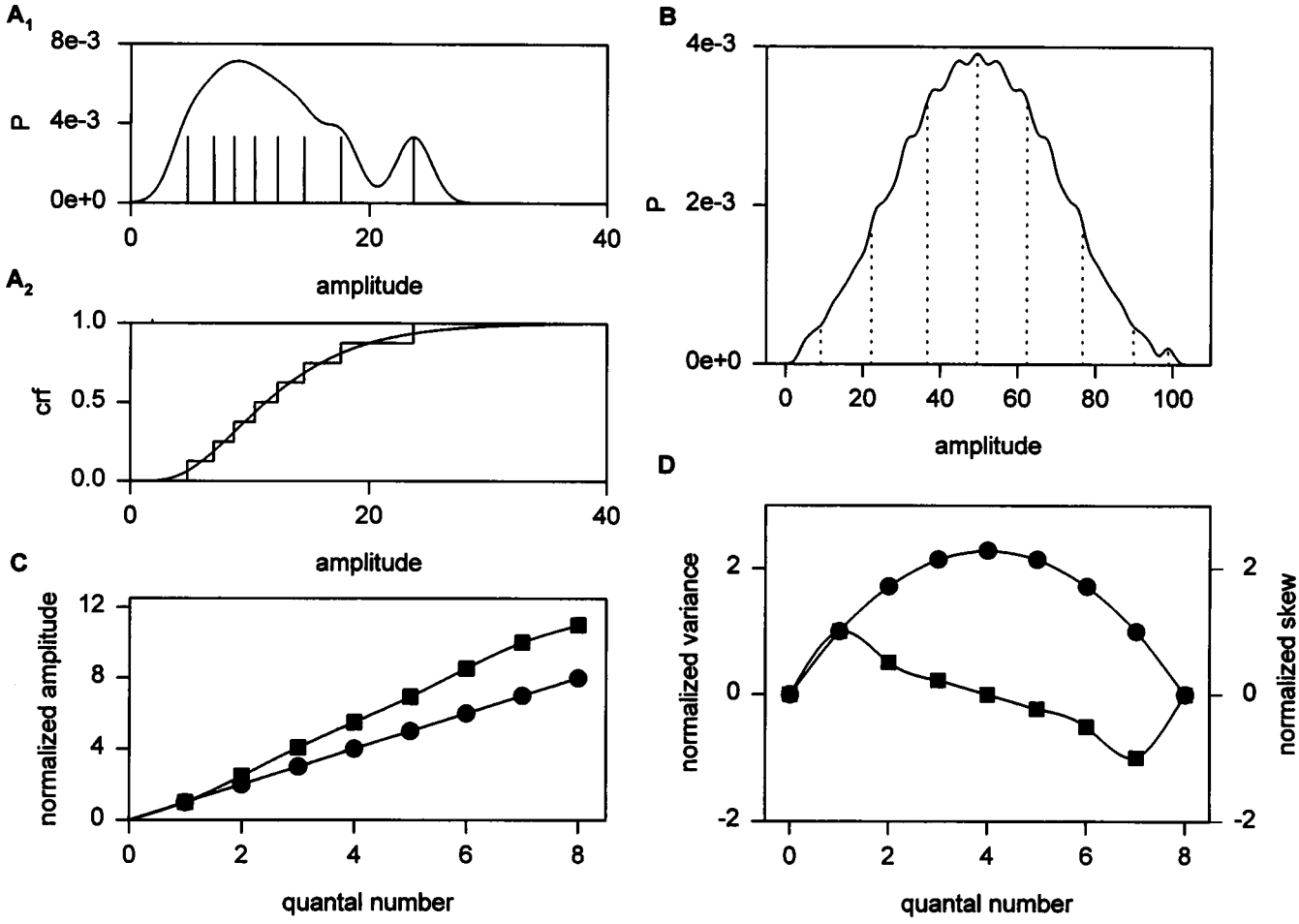

FIGURE 2 The effects of variance in mini amplitude that are due to differences between sites. (A_1) A mini distribution generated by differences between sites is generated for a cell with eight release sites (drop lines). Although the underlying distribution is discrete, convolution of simulated gaussian noise (continuous distribution) over the drop lines causes the individual contributions of each site to overlap, making peaks difficult to resolve at small amplitudes. The y axis has been scaled to the post-convolution distribution for both cases. (A_2) A comparison of the unconvolved distribution in A_1 and the mini distribution in Fig. 1 *A* using cumulative relative frequencies. The maximum difference between distributions is about 6%, and in practice it would be hard to separate the two without a very large sample size. (*B*) The distribution of synaptic current amplitudes expected when each of the eight release sites has a probability of release of 0.5 and is associated with one of the discrete size classes shown in A_1. The resultant distribution has been convolved with noise to allow hundreds of individual resultant combinations of amplitude, each of which represents a discrete amplitude, to overlap. Failures to release by all sites have again been excluded. Drop lines represent mean amplitude at each quantal number. Although small peaks are visible in this distribution, they bear no relation to quantal peaks. (*C*) The normalized mean (●) of each quantal peak increases linearly with quantal number with a slope of 1; the normalized mode (■) increases with quantal number in a nonlinear fashion. Means and modes are normalized as in Fig. 1 *C*. (*D*) The variance of each quantal peak (●) is parabolically dependent on quantal number, as predicted by Jack et al. (1994), and the skew of each quantal peak (■) is symmetrical around $q = 4$, half the maximum number of quanta released.

having a standard deviation of 1.5. The discrete distribution has equal frequencies of release at each site, but convolution of noise onto this distribution gives the continuous distribution a mode. Although the distributions generated by variance within and between sites are completely different in their underlying statistical description, even without taking baseline noise into consideration, a sample size of more than 400 is required to distinguish between them with 95% confidence by the model-independent Kolmogorov-Smirnov test (Fig. 2 A_2).

The distribution of responses at a given quantal number, q, can be constructed from the amplitudes and relative frequencies of all of the possible discrete amplitudes generated by sampling from the unconvolved distribution in Fig. 2 A_1, without replacement, q times. By combining the distributions for each quantal number and convolving with noise, the distribution of evoked synaptic current amplitudes predicted by a binomial release process with the same parameters as Fig. 1 *B* ($N = 8$, $p = 0.5$) can be generated; this is shown in Fig. 2 *B*. Peaks in amplitude are apparent with large enough sample size; however, the eight quantal peaks, each representing an integer multiple of quanta, are obscured because the variance of the mini distribution causes the set of discrete amplitudes composing each quan-

tal peak to overlap with the set of discrete amplitudes of neighboring quantal peaks. The observable peaks represent the chance summation of two or more of the possible discrete amplitudes from different quantal peaks. The total number of possible discrete amplitudes can be calculated by combinatorial statistics from Eq. 1:

$$C = \sum_{q=1}^{N} \frac{N!}{q!(N-q)!}, \quad (1)$$

where C is the total number of discrete amplitudes and q is the number of quanta released. For $N = 8$, there are 309 possible discrete amplitudes in the multiquantal distribution. The summation of these discrete amplitudes is what generates the peaks observed in the total distribution, and these peaks are uninterpretable when one is attempting to recover information about the parameters underlying quantal release.

As is the case when variance occurs within sites, the mean of each quantal peak increases linearly and in equal increments with quantal number (Fig. 2 *C*, *circles*), but unlike the previous case, the variance of each quantal peak is parabolically related to the quantal number (Fig. 2 *D*, *circles*). This is because of the lack of replacement during sampling of the distribution of mini amplitudes per release site. The lack of replacement also affects the skew of the quantal peaks. The skews at low and high quantal number are symmetrical around zero, and when half the total number of quanta are released, there is no skew in the resultant quantal peak (Fig. 2 *D*, *squares*). As is the case when variance occurs within sites, the relationship between skew and quantal number causes the modes of the quantal peaks to be nonquantally separated (Fig. 2 *C*, *squares*). The effects of differences between sites on both the variance and the skew of quantal peaks can be understood by considering that when all variance in mini amplitude occurs between release sites, release from a single site generates a distribution that is the mirror image of the distribution generated by release from all sites but one.

In summary, a skewed mini distribution with variance generated entirely by differences between sites causes a discrete distribution of multiquantal amplitudes. As is the case for variance intrinsic to each site, the mean amplitude of each quantal peak increases linearly with increasing quantal number, and the modes are nonquantally separated. However, the variance of each quantal peak is parabolically related to quantal number and the shape of each quantal peak depends on how far that peak is from the half-maximum quantal number. Furthermore, the size classes associated with a single quantal number overlap substantially with the size classes of neighboring quantal numbers, making the quantal peaks unresolvable.

The consequences of a low probability of release

Our results to this point suggest that, unless the mini distribution is much broader than the uniquantal distribution, quantal peaks will be unresolvable, regardless of the source of variance in mini amplitude. It might reasonably be argued, however, that this is a result of our choice of a low N and a high p, so that only rarely would trials result in the release of just one or two quanta. Because the first few peaks of the PDF generally have the smallest variance, our de-emphasis of the first few peaks will inevitably bias our results toward an inability to resolve quantal peaks. To find out if this bias compromises the generality of our conclusions, we briefly consider a circumstance in which N is large and p is small (the Poisson limit), and in which the first few peaks are the major constituents of the PDF of evoked responses.

A consequence of having N high and p low is that the source of mini amplitude variance has little effect on the expected evoked amplitude PDF. This is because, with p small, the chance of any one of the large number of release sites contributing to an evoked response is not substantially affected by the lack of replacement implied by variance in mini amplitude between sites. To illustrate this point, we show in Fig. 3 the expected relationships between the evoked response variance and the number of quanta released when N is 100. When variance in mini amplitude is intrinsic to each site, the increase in normalized response variance with increasing quantal number is linear, with a slope of 1 (*solid line*, Fig. 3 *A*). When variance in mini amplitude occurs between sites, the normalized variance is parabolically related to the quantal number, with an initial slope of 1 and a second x axis intercept at $q = 100$ (*dotted line*, Fig. 3 *A*). Although these effects are similar to those considered in Figs. 1 and 2, when only the first eight quantal peaks are considered, the relationship between variance and quantal number is only slightly dependent on the model used (Fig. 3 *B*). If the Poisson limit applies and only the first few quantal peaks are apparent, the two models can be treated identically.

Using the mini distribution from Fig. 1 *A*, we have performed simulations giving particular Poisson distributions, and in no case was it possible to discern quantal peaks. Rather than explore all possible Poisson distributions in search of a case where peak resolution might be possible, we suggest instead that the ability to resolve peaks will never be greater than if the first two peaks are of equal height and no other modes are present. This condition is illustrated in Fig. 3 *C*, where the sum of the peaks (*solid line*) makes it clear that the component peaks (*dotted lines*) would be unresolvable, even under this most favorable circumstance. This result argues strongly that our conclusions about the resolvability of peaks are not special to the case of low N and high p, but for completeness we have also considered the case where N is low ($N = 8$), and all variance in mini amplitude occurs between sites, but only the first two quantal peaks are considered. Under these conditions, which are heavily biased toward quantal peak resolution, the two simulated peaks are again unresolvable but, as in Fig. 2 *B*, there are peaks apparent in the simulated PDF, although they do not correspond to the modes of either quantal peak (not shown).

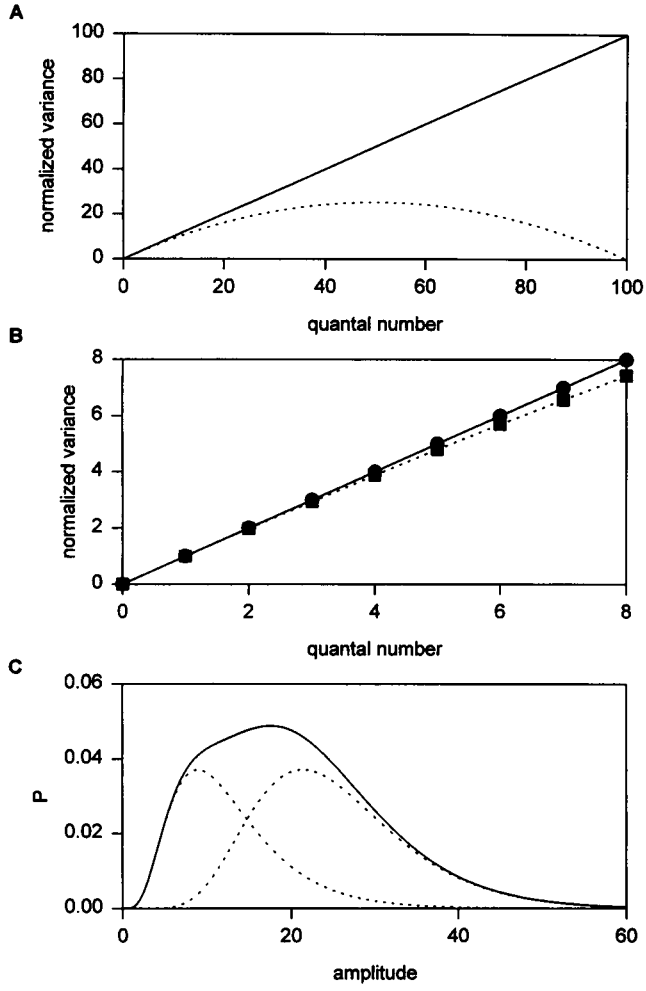

FIGURE 3 At the Poisson limit, quantal peaks are independent of the source of mini amplitude variance and are not resolvable. (*A*) The two different models are compared when $N = 100$: variance in mini amplitude that is intrinsic to each site causes a linear increase in the variance of each quantal peak as quantal number increases (*solid line*; see Fig. 1 *D*, *circles*), whereas variance in mini amplitude that is due to differences between sites causes a parabolic relationship between the variance of each quantal peak and quantal number (*dotted line*; see Fig. 2 *D*, *circles*). Because of the very large number of possible size class combinations when differences occur between sites and $N = 100$, the parabola was constructed by best second-order fit to three points: $q = 0$, normalized variance = 0; $q = 1$, normalized variance = 1; and $q = 100$, normalized variance = 0. (*B*) An enlargement of the area in *A* that corresponds to the first eight quantal peaks. Key as in *A*. Note that for small quantal numbers, the variance of the associated quantal peak is nearly identical for both models. (*C*) The first two quantal peaks generated as in Fig. 1 *A* are normalized to the same size (*dashed lines*) and summed together (*solid line*) to form a distribution that is not resolvably bimodal.

A general description of the effects of variance in mini amplitude on variance in stimulus-evoked current amplitude

Because our simulations suggest that quantal peaks are obscured during stimulus-evoked release if the uniquantal distribution is similar to the mini distribution, regardless of which model for variance in mini amplitude applies, we feel that it is unsafe to use a theoretical framework for analyzing stimulus-evoked data that depends on the accurate resolution of quantal peaks. We have therefore restricted ourselves to a consideration of the stimulus-evoked mean and variance, two parameters that can be measured directly in a model-independent fashion. This approach has the additional advantage that small sample sizes yield reasonably accurate measurements of the mean and variance, which in practice allows shorter experimental collecting periods and reduces the risk of nonstationarity.

A general description of the statistical properties of a population of stimulus-evoked release can be derived by considering each release site individually and then expanding to all release sites simultaneously. Given the initial conditions that each release site x produces minis of mean amplitude μ_x and variance σ_x^2 and releases a quantum in response to stimulation with a probability p_x, the variance in evoked current amplitude at that site will be (Kullman, 1994)

$$\sigma_{e,x}^2 = p_x(1 - p_x)\mu_x^2 + p_x\sigma_x^2 . \quad (2)$$

This equation can be expanded to

$$\sigma_{e,x}^2 = p_x\mu_x^2 - p_x^2\mu_x^2 + p_x\sigma_x^2 . \quad (3)$$

For the sake of simplicity, we will assume that all sites have the same intrinsic variance in mini amplitude σ_i^2. Considering all N sites simultaneously, the variance in evoked amplitude will be

$$\sigma_e^2 = \sum_{x=1}^{N} p_x\mu_x^2 - \sum_{x=1}^{N} p_x^2\mu_x^2 + \sum_{x=1}^{N} p_x\sigma_i^2 , \quad (4)$$

and the expected variance in evoked amplitude, $E(\sigma_e^2)$, can be described in terms of the expected values of each sum:

$$E(\sigma_e^2) = NE(p_x\mu_x^2) - NE(p_x^2\mu_x^2) + N\sigma_i^2E(p_x) . \quad (5)$$

The expected value of a product of two variables is equal to the product of the expected values of the two variables plus the covariance between them, so

$$E(\sigma_e^2) = N[E(p_x)E(\mu_x^2) + \mathrm{Cov}(p_x, \mu_x^2)] - N[E(p_x^2)E(\mu_x^2) + \mathrm{Cov}(p_x, \mu_x^2)] + N\sigma_i^2E(p_x) . \quad (6)$$

This equation can be rearranged to give

$$E(\sigma_e^2) = NE(\mu_x^2)[E(p_x) - E(p_x^2)] + N\sigma_i^2E(p_x) + N[\mathrm{Cov}(p_x, \mu_x^2) - \mathrm{Cov}(p_x^2, \mu_x^2)] . \quad (7)$$

The expected value of a squared variable is equal to the sum of the variance of that variable and the squared expected

value of that variable, so the expected variance in evoked amplitude is

$$E(\sigma_e^2) = N((\sigma_{\mu_x}^2) + E(\mu_x)^2)[E(p_x) - (\sigma_{p_x}^2 + E(p_x)^2)] + N\sigma_i^2 E(p_x) + N[\mathrm{Cov}(p_x, \mu_x^2) - \mathrm{Cov}(p_x^2, \mu_x^2)], \quad (8)$$

where $\sigma_{p_x}^2$ is the variance in p_x and $\sigma_{\mu_x}^2$ is the variance in μ_x. The expected value of a variable is its mean, so by using the overhead bar as the notation for the mean value of a variable, Eq. 7 can be equivalently stated as

$$\overline{\sigma_e^2} = N(\sigma_{\mu_x}^2 + \bar{\mu}_x^2)[\bar{p}_x - (\sigma_{p_x}^2 + \bar{p}_x^2)] + N\sigma_i^2\bar{p}_x + N[\mathrm{Cov}(p_x, \mu_x^2) - \mathrm{Cov}(p_x^2, \mu_x^2)], \quad (9)$$

and this equation can be rearranged to give a form resembling the classical description of variance in evoked current amplitude:

$$\overline{\sigma_e^2} = N\bar{p}_x\left[1 - \bar{p}_x - \frac{\sigma_{p_x}^2}{\bar{p}_x}\right](\sigma_{\mu_x}^2 + \bar{\mu}_x^2) + N\bar{p}_x\sigma_i^2 + N[\mathrm{Cov}(p_x, \mu_x^2) - \mathrm{Cov}(p_x^2, \mu_x^2)]. \quad (10)$$

The covariance terms in Eq. 10 are nonzero if the amplitude at a site is related to the probability of release at that site, a constraint that we consider plausible. However, the difference between the two covariance terms in Eq. 10 has little intuitive value; to illustrate the meaning of this difference, we rewrite Eq. 10 using the useful identity $\mathrm{Cov}(x, y) + \mathrm{Cov}(z, y) = \mathrm{Cov}(x + z, y)$:

$$\mathrm{Cov}(p_x, \mu_x^2) - \mathrm{Cov}(p_x^2, \mu_x^2) = \mathrm{Cov}(p_x - p_x^2, \mu_x^2) = \mathrm{Cov}(\sigma_{r,x}^2, \mu_x^2), \quad (11)$$

where $p_x - p_x^2$ is equal to the variance in the occurrence of release at each site x, $\sigma_{r,x}^2$. Whereas we consider a relationship between p_x and μ_x possible, a relationship between $\sigma_{r,x}^2$ and μ_x seems much less likely, and we therefore consider it likely that this covariance term will be equal to or close to zero. Neglecting this term, Eq. 10 reduces to

$$\overline{\sigma_e^2} = N\bar{p}_x\left[1 - \bar{p}_x - \frac{\sigma_{p_x}^2}{\bar{p}_x}\right](\sigma_{\mu_x}^2 + \bar{\mu}_x^2) + N\bar{p}_x\sigma_i^2. \quad (12)$$

Although this equation is general and broadly applicable, it is cumbersome and requires knowledge of σ_p^2. We therefore consider the limiting case where the probability of release is uniform at all sites:

$$\overline{\sigma_e^2} = Np(1 - p)(\sigma_{\mu_x}^2 + \bar{\mu}_x^2) + Np\sigma_i^2. \quad (13)$$

We cannot directly measure $\sigma_{\mu_x}^2$, $E(\mu_x)$, or σ_i^2, so we will redefine these variables in terms of the mean and variance of the whole cell mini distribution, μ_m and σ_m^2, respectively. If each release site contributes with equal frequency to the whole cell mini distribution, $E(\mu_x)$ is equal to the mean mini amplitude measured from the whole cell distribution. The sources of variance in the mini distribution, σ_i^2 and $\sigma_{\mu x}^2$, sum to produce the total variance σ_m^2, so we define a variable, W, as the fraction of total variance in mini amplitude that is due to variance intrinsic to each site. The expected variance in evoked responses can now be described in terms of N, p, W, μ_m, and σ_m^2:

$$\overline{\sigma_e^2} = Np(1 - p)[\mu_m^2 + (1 - W)\sigma_m^2] + NpW\sigma_m^2. \quad (14)$$

Note that in the limiting case where all variance in mini-amplitude occurs within sites, this equation reduces to one given elsewhere (Bekkers and Stevens, 1990; Borges et al., 1995):

$$\overline{\sigma_e^2} = Np(1 - p)\mu_m^2 + Np\sigma_m^2, \quad (15)$$

and in the case where all variance in mini amplitude occurs between sites, the expected evoked variance is

$$\overline{\sigma_e^2} = Np(1 - p)(\mu_m^2 + \sigma_m^2). \quad (16)$$

To test the validity of Eq. 14, we performed Monte Carlo simulations in which the relative contributions of each source of variance in mini amplitude were varied and the expected variance in evoked responses was measured. As shown in Fig. 4, the mean evoked variance is not significantly different from the value predicted by Eq. 14, confirming its utility.

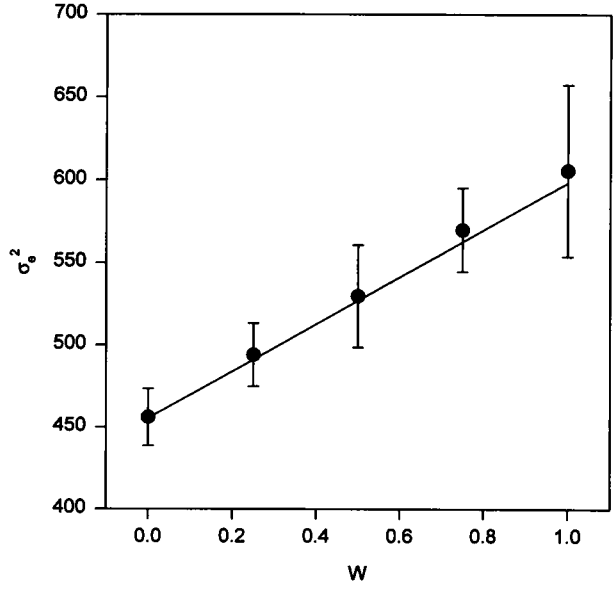

FIGURE 4 Validation of Eq. 14 by Monte Carlo simulation. Simulated mini distributions were generated by combining different fractions of variance due to intrinsic factors and differences between sites. The variable W represents the fraction of total variance in mini amplitude that is intrinsic to each site. The total variance in mini amplitude was in all cases constrained to have the same numerical value. Each site was assumed to have a probability of release of 0.5 for each trial, and a total of 500 trials were run in each simulated experiment. A total of 10 experiments at each point were run, and the average evoked variance was plotted (●), along with the standard deviation of the evoked variance (*error bars*). The line represents the theoretical predictions from Eq. 14.

To be useful, the mathematical description of $E(\sigma_e^2)$ as a function of W must give us predictions that we can then use to determine N, p, and W. Fig. 5 shows a comparison of the mean value of evoked variance as a function of p in the limiting cases where $W = 0$ and where $W = 1$. When p is low, the two models are difficult to distinguish, but when p is high, differences are readily apparent and are greatest when $p = 1$. Unfortunately, the only parameters from Eq. 14 that can be directly measured from the mini distribution and evoked distribution are μ_m and σ_m^2. $E(\sigma_e^2)$ can be approximated by a measured single value for σ_e^2, but N, p, and W are all unknown, and more information is needed to unambiguously solve this equation for the parameters of interest. We therefore turn next to the mean evoked response.

The expected mean evoked response, $E(\mu_e)$, can be derived in a manner similar to that described above; the equation relating $E(\mu_e)$ to the above parameters is (Borges et al., 1995)

$$\bar{\mu}_e = Np\mu_m. \tag{17}$$

Note that this equation is independent of W, and $E(\mu_e)$ can be approximated by a measured single value for μ_e. Eqs. 14 and 17 use all of the model-independent information that can easily be obtained under most experimental conditions, but this still leaves a total of three unknowns. Because there are more variables than equations, we cannot obtain a unique solution for N, p, or W without an independent estimate of one of those parameters. However, we can place limits on the error that the third variable, W, causes in estimates of N and p, because the values for W are restricted to being between 0 and 1.

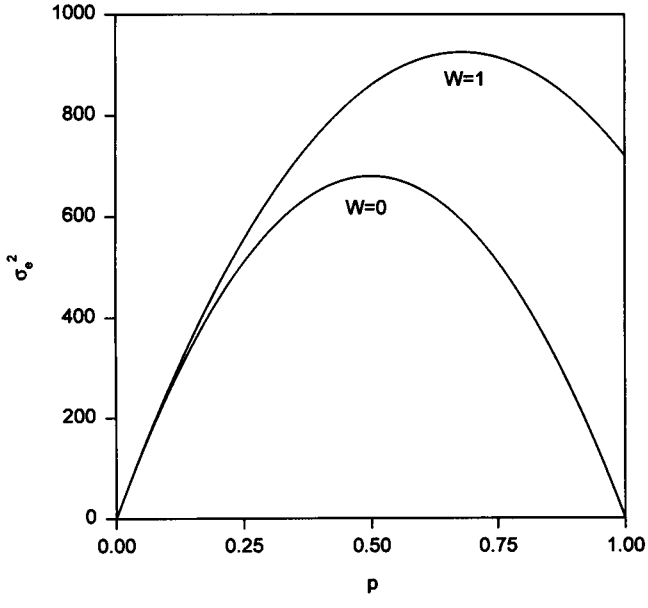

FIGURE 5 The relationship between the expected variance in amplitude of evoked currents and the probability of release when $W = 1$ (all mini amplitude variance occurs within each site) and when $W = 0$ (all mini amplitude variance occurs between sites) as predicted by Eq. 14. $N = 20$, $\mu_m = 10$, and $\sigma_m^2 = 36$. When $W = 0$, the relationship between p and variance in amplitude of evoked currents is a parabola that intersects the p axis at $p = 0$ and $p = 1$; the variance at $p = 1$ is zero because the quantum at each site is invariant, and each site invariably releases a quantum. When $W = 1$, the relationship is the sum of a line and a parabola (see Eq. 15); although the sum of a line and a parabola is simply another parabola (see Fig. 7), this new parabola only intersects the p axis once for the range of real values of p, because even when each site releases a quantum invariably ($p = 1$), the quanta released vary in amplitude from one trial to the next.

Limits on the errors in estimating N and p caused by an unknown value of W

In previous work on cultured amacrine cells, quantal GABA release was evoked by depolarizations of the presynaptic cell to 0 mV lasting 30 ms or longer, and the trial-to-trial variance in the postsynaptic $GABA_A$ receptor-mediated response was determined (Borges et al., 1995). $GABA_A$ receptor-mediated minis evoked by long-lasting depolarizations to around −35 mV were also recorded in the same cells, and Eq. 15 was used to solve for N and p by assuming all variance in mini amplitude to be intrinsic to each site. With this assumption, p was found to lie close to 1 for the peak postsynaptic current. This conclusion was supported by independent estimates of the release rate, which showed an apparent spike of release that rapidly decayed to a low steady-state level, even during the depolarization protocol, consistent with a model of release in which each site rapidly releases a vesicle and is then rate-limited by reloading of another vesicle (Borges et al., 1995).

A model-independent restatement of the conclusion that p is at or near 1 if W is 1 is that the ratio $(\mu_m\sigma_e^2)/(\mu_e\sigma_m^2)$ is approximately equal to 1 (see Eq. 15). We now reexamine the data from Borges et al. (1995) with our more general expression to determine how much error in the original estimates of N and p could be generated by relaxing the assumption that all variance in mini amplitude is intrinsic to individual release sites.

Eqs. 17 and 14 can be combined to produce a relationship between observed data, W, and p:

$$p = 1 - \frac{\dfrac{\mu_m\overline{\sigma_e^2}}{\bar{\mu}_e} - W\sigma_m^2}{\mu_m^2 + (1 - W)\sigma_m^2}. \tag{18}$$

We can combine this equation with the experimental observation that $(\mu_m\sigma_e^2)/(\mu_e\sigma_m^2) = 1$ to produce a simplified equation relating W and p:

$$p = 1 - \frac{1}{\dfrac{\mu_m^2}{(1 - W)\sigma_m^2} + 1}. \tag{19}$$

This equation can be restated using the CV of the mini-distribution, $CV_m = \sigma_m/\mu_m$:

$$p = 1 - \frac{1}{\dfrac{1}{(1 - W)CV_m^2} + 1}. \tag{20}$$

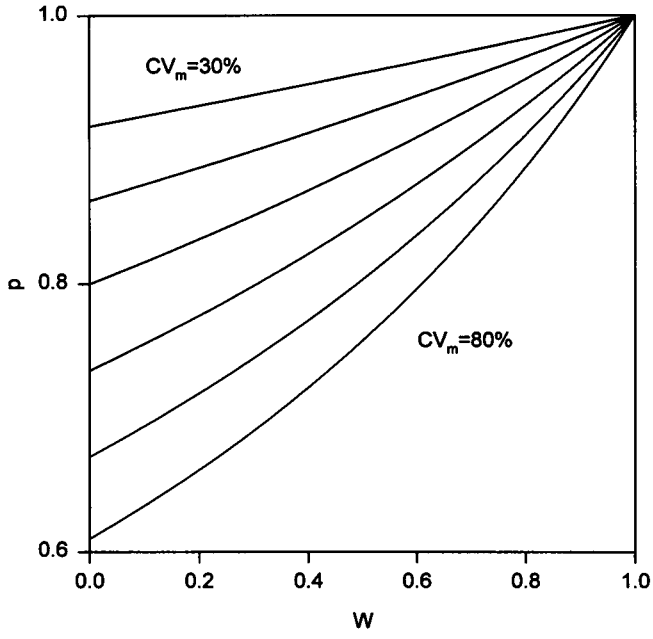

FIGURE 6 The value for p calculated by Eqs. 14 and 17 is dependent on the assumed value for W. The relation between p and W required to reproduce the experimentally observed $(\mu_m\sigma_e^2)/(\mu_e\sigma_m^2) = 1$ for different CVs for the mini distribution is shown as calculated by Eq. 20. The CV of the mini distribution varies from 30% (*top*) to 80% (*bottom*) in 10% increments. The error in the calculated value for p is between roughly 20% and 35% for CVs in the range 50–70%, as commonly observed at central synapses.

The error in p caused by an incorrectly assumed value for W can now be determined analytically. The relationship between W and p is shown in Fig. 6 for a range of CV values for the mini distribution, and as the CV of the mini distribution increases, so does the error in p. Using the data from Borges et al. (1995), we calculate the p values, assuming $W = 0$ to average 0.80 ± 0.07 ($n = 7$). If the value for W is completely unconstrained, therefore, the probability of release lies somewhere between 0.8 and 1.

In a recent analysis using the observation that two neurons can sometimes respond to the same quantum of transmitter, we have estimated that a minimum of roughly 75% of the variance in mini amplitude is due to trial-to-trial fluctuations in mini amplitude (Frerking et al., 1995). These data constrain the value for W in these cells to be between 0.75 and 1. Taking 0.75 as a lower limit for W reduces the error in p substantially; the average p value calculated when W is 0.75 in these cells is 0.93 ± 0.05 ($n = 7$).

Changes in *N*, *p*, and *A* can be identified, regardless of the value of *W*

In Fig. 5 we demonstrated that the relationship between p and variance in evoked responses differs, depending on the value of W. Unfortunately, this cannot be used to determine W, because only the product $N \cdot p$, given by μ_e/μ_m, is measurable (see Eq. 17). We demonstrate here that given the model-independent parameters of the mini distribution and evoked distribution, the relationship between variance in evoked responses and the $N \cdot p$ product is independent of the source of variance in mini amplitude. A useful implication of this is that changes in N, p, and A can be detected, regardless of the source of variance in mini amplitude.

Fig. 7 shows the relationship between evoked current variance and the $N \cdot p$ product under two conditions: first, where the means and variances of the mini distribution and the evoked distribution are used to solve N and p, assuming all variance occurs between sites ($W = 0$; *dotted line*); and second, where the same information is used to solve N and p, assuming all variance occurs within sites ($W = 1$; *solid line*). Amazingly, the parabolic relationship between evoked variance and the $N \cdot p$ product is the same under both conditions. This is because the initial slope of the parabola is independent of W, as we will demonstrate below, and the point representing the measured evoked responses, which is elsewhere along the parabola with coordinates determined by μ_e/μ_m and σ_e^2, is constrained to be the same in both cases. The initial slope and one point outside of the region of low $N \cdot p$ values are all that is required to reproduce the

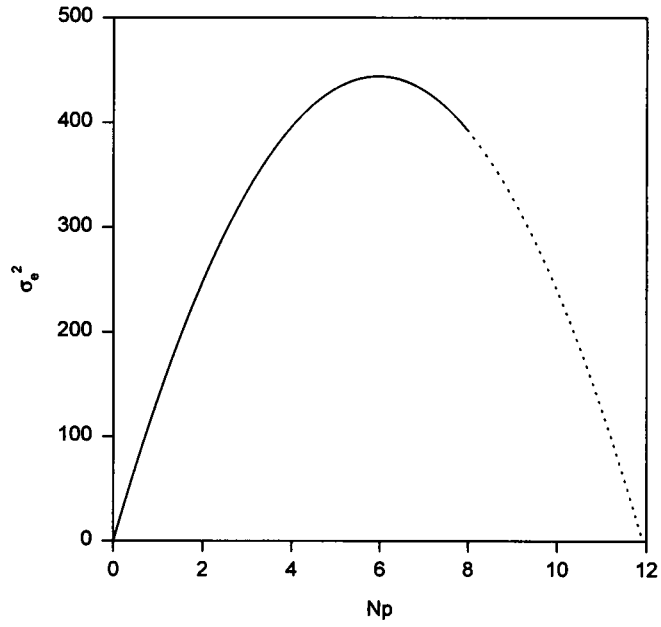

FIGURE 7 The relationship between the $N \cdot p$ product and the expected variance in amplitude of evoked current is parabolic, regardless of the value of W. The curves shown are for $N = 8$ and $W = 1$ (——), and when $N = 11.92$ and $W = 0$ (· · · ·). The values of N when $W = 1$ and when $W = 0$ that produce the same parabola were determined using Eqs. 18 and 17. $\mu_m = 10$ and $\sigma_m^2 = 49$. The expression when $W = 1$ does not extend back down to the $N \cdot p$ axis when $p = 1$ for reasons outlined in the Fig. 5 legend. However, because the equation relating $N \cdot p$ to variance in amplitude of evoked currents is a parabola independent of the value for W (see Fig. 5 legend), the same parabola can be produced on the axes shown here for all values of W by specific combinations of W and N. The only difference between the relationships at different values of W is how far they extend back toward the $N \cdot p$ axis when $p = 1$, and so only if W is low and p is very high can high values of W be ruled out.

entire parabola, and so the parabolas at different values of W are constrained to be the same.

The initial slope is independent of W because Eq. 14 can be expanded and simplified to

$$\overline{\sigma_e^2} = -Np^2(\mu_m^2 + (1 - W)\sigma_m^2) + Np(\mu_m^2 + \sigma_m^2). \quad (21)$$

Because for low values of $N \cdot p$, p is small and p^2 becomes negligible, this equation reduces to one independent of W:

$$\overline{\sigma_e^2} = (\mu_m^2 + \sigma_m^2)Np. \quad (22)$$

Of course, the independence of the relationship between σ_e^2 and $N \cdot p$ from W does not imply that the values of N and p are independent of W. Using Fig. 7 to illustrate this point, we consider the point that is equal to $p = 1$ when $W = 1$; on the $N \cdot p$ axis, this corresponds to a value of 8, implying eight release sites, each with a probability of release of 1. If $W = 0$, the same position on the $N \cdot p$ axis implies around 12 release sites, each with a probability of release of about 0.67. This effect is predicted by Eq. 18. Another way of expressing this general result is to say that for any relationship between $N \cdot p$ and the variance of evoked current that can exist when $W = 1$, there is a unique combination of N and p for every other value of W that matches this relationship.

The result that the parabola relating σ_e^2 to $N \cdot p$ is unchanged by the values for W allows us to suggest a method relevant to studies of synaptic plasticity that can detect changes in N, p, or A. Providing that conditions are satisfied where Eq. 14 is valid, it should be possible to construct a parabola, like that in Fig. 7, before a change in synaptic strength. All that is required to construct this parabola are the mean and variance of the mini distribution, which by Eq. 22 can be used to give the initial slope, and a point whose position on the $N \cdot p$ axis is determined by the ratio μ_e/μ_m (Eq. 17). After a change in synaptic strength a new point can be plotted; only if the change in synaptic strength occurs solely through a change in p will the new point fall on the previously described parabola. If N has changed, the initial slope will be unchanged, but the new point will fall off the previously described parabola. If A has changed, the initial slope of the parabola will have changed.

DISCUSSION

A comparison of models: differences in quantal peaks

One of the purposes of this work was to determine the effects of variance in mini amplitude on stimulus-evoked release for two conditions: when the variance in mini-amplitude is due to trial-to-trial fluctuations in amplitude at every site, and when the variance in mini amplitude is due to differences in amplitude between release sites. We have demonstrated that, using a description of a mini distribution typical for central neurons, the modes, variances, and skews of quantal peaks in stimulus-evoked currents are expected to show substantial differences, depending on which condition applies. Quantal peaks will, in practice, be unresolvable if the mini distribution corresponds to the uniquantal distribution, because, even though variance in mini amplitude occurring between sites reduces the variance of multiquantal peaks when compared to the alternative case when all variance in mini amplitude occurs within sites, this effect is not large enough by itself to allow quantal peak resolution. This result is robust under conditions of high N and low p, and low N and high p. It is therefore unlikely that the number of events in each quantal peak, or indeed even the number of quantal peaks, could be accurately determined under most experimental conditions if the mini amplitude distribution corresponds to the distribution of uniquantal events.

In performing the analysis described here we have based our simulations on data from our own work on cultured amacrine cells (Frerking et al., 1995). To determine whether this analysis is relevant to studies of mammalian central synapses, we examine points of similarity and difference. Like the mini distributions of our amacrine cells, the mini-distributions of numerous central neuronal types in culture and in slices show a positive skew and large variance (Bekkers and Stevens, 1990; Edwards et al., 1990; Manabe et al., 1992; Silver et al., 1992; Otis and Mody, 1992; Rekling, 1993; Ulrich and Lüscher, 1993; Wyllie et al., 1994; De Koninck and Mody, 1994; Tang et al., 1994; Tong and Jahr, 1994; Jonas et al., 1993; Frerking et al., 1995). The CV of the mini distribution from mammalian central neurons is generally not reported, but we have calculated the CVs for many of these systems (Edwards et al., 1990; Manabe et al., 1992; Silver et al., 1992; Ulrich and Lüscher, 1993; Wyllie et al., 1994; De Koninck and Mody, 1994; Tang et al., 1994; Jonas et al., 1993) from published histograms of mini amplitude. We find that the CVs in these central neurons range from around 44% (Silver et al., 1992, Fig. 2 *D*) to around 93% (Jonas et al., 1993, Fig. 12) with a mean of 59 ± 16% ($n = 8$), indicating that our amacrine cells are not atypical in their coefficients of variation. It is likely also that the normal experimental conditions in recent studies using quantal analysis (Edwards et al., 1990; Larkmann et al., 1991; Jonas et al., 1993) are comparable to those we have simulated. In these studies, the mean number of quanta released is typically in the range of 3–8, so either high N and low p, or low N and high p must be the case, but as we show (Fig. 3 *B*), only in the latter case is there a difference between the models for variance in mini amplitude, and in neither case is quantal peak resolution expected if the uniquantal distribution is similar to the mini distribution.

This conclusion that quantal peaks in histograms of evoked data ought to be unresolvable if the mini distribution is analogous to the uniquantal distribution leads to an important question. If the frequently observed peaks in histograms of evoked currents or voltages are not based on integer multiples of the observed mini distribution, what are they? It is not our purpose here to exhaustively list possible

reasons for peaky data, but we consider three possibilities for which mechanisms have recently been proposed. The first possibility is that the mini distribution is "subquantized," because of multivesicular release at a single site (Bekkers and Stevens, 1994) or quantization of postsynaptic receptor number (Edwards et al., 1990). If this is the case, equally separated peaks in the data would likely be due to this subquantal nature of transmission; although these peaks would reveal little useful information for determining N, p, W, or A, they would restrict models explaining variance in mini amplitude to those having a physical explanation of subquanta.

The second possibility is that the mini distribution contains a significant number of multiquantal events, as might be expected if the probabilities of release at different sites are nonindependent (Korn et al., 1993, 1994; Edwards, 1995). However, even if this does occur, quantal peak resolution is not expected to be any better in the stimulus-evoked distribution than in the mini distribution. This point makes it unlikely in practice that this effect could allow stimulus-evoked quantal peaks to be resolved, because even in those studies that claim the mini distribution has multiquantal events, the putative multiquantal peaks in the mini-distribution are not well separated (Edwards et al., 1990; Korn et al., 1993; Ulrich and Lüscher, 1993; Korn et al., 1994), and there is still debate over whether this peakiness is truly due to multiquantal events, or to sampling error from a non-normal but unimodal distribution (Bekkers and Stevens, 1994).

A third explanation for quantal peaks, proposed in several recent studies (Jonas et al., 1993; Jack et al., 1994; von Kitzing et al., 1994), is that although the mini distribution might be a uniquantal distribution, it has a larger variance than the stimulus-evoked uniquantal distribution. This is possible because minis are generally spontaneous and are therefore not restricted solely to the set of synapses being stimulated. In the most extreme case, different presynaptic inputs might have characteristic and different uniquantal sizes; the mini distribution would include events from multiple inputs and so would have a large variability in amplitude, but the stimulus-evoked events, all being from a single input, would have much less variability. There is indirect support for this extreme case (Sorra and Harris, 1993), but it is unlikely to be generally significant for two reasons. First, the mini distributions of isolated cells in culture, where the number of inputs is frequently 1 (Bekkers and Stevens, 1991; Tong and Jahr, 1994; Bekkers and Stevens, 1995; Borges et al., 1995; Frerking et al., 1995), show roughly the same large variance as that observed in slices. Second, when the uniquantal distributions of two separate inputs onto the same postsynaptic cell at CA3-CA1 synapses in hippocampal slices are isolated by a desynchronizing evoked release (see below) and compared, they are not resolvably different (Oliet et al., 1996). Both this extreme case and the less extreme case, that the uniquantal distribution from the set of stimulated synapses has less variance than do other synapses from the same presynaptic cell, are unlikely on the basis of three additional experimental results. First, experiments in which minis and evoked responses have been locally stimulated from the same region of a dendrite in culture suggest that mini amplitude distributions at the sites contributing to the evoked responses have large variances and positive skews (Bekkers and Stevens, 1995). Second, in some experiments in culture, minis are not spontaneous but rather are evoked by depolarization, and yet they still show a large variability in amplitude (Borges et al., 1995; Liu and Tsien, 1995; Frerking et al., 1995). Third, bath application of Sr^{2+} or low concentrations of Cd^{2+} desynchronize or reduces release and are thought to allow the uniquantal events during stimulus-evoked release from cells in slices to be directly measured. Like the mini distributions from the same cell types, these uniquantal distributions show a large variance and skew toward large events at both the endbulb of Held (Isaacson and Walmsley, 1995) and CA3-CA1 synapses (Bekkers, 1995; Oliet et al., 1996). We note that the results described here from cultured neurons could conceivably be attributed to possible artifacts associated with tissue culture; however, the experimental approaches used on cells in slices generated the same conclusion, making this possibility less likely.

Independent of whether the uniquantal distribution is identical with the mini distribution, our simulations have a number of implications for quantal analysis. First, even if quantal peaks are unresolvable, differences between sites can give rise to peaks in the data that could be fitted, incorrectly, to models assuming them to be quantal peaks. Second, if the uniquantal distribution is skewed, as is the mini distribution, each quantal peak is expected to have a different shape, regardless of whether the mini amplitude variance occurs within or between sites. Because of this, fits to data using gaussians to model the quantal peaks will be in error. This is particularly relevant because gaussians are almost exclusively used for complex fitting techniques such as maximum likelihood estimation, even in studies where the mini distribution in the same cells is obviously non-normal (Edwards et al., 1990; Jonas et al., 1993). Finally, we expect that any skew in the uniquantal distribution will cause the modes of each quantal peak to be separated by unequal amounts, regardless of the model for variance in amplitude. Because the modes of the distributions represent the part of each quantal peak that will be easiest to resolve, a nonquantal separation of the visible peaks in stimulus-evoked data is expected, and equations constraining peaks to be quantally separated will fit the data incorrectly.

Solving for quantal parameters without resolving quantal peaks: the effects of sources of variance in mini amplitude

Because our simulations predict that quantal peaks are not readily resolvable whether variance in mini amplitude occurs within sites or between them, provided that the uni-

quantal distribution is approximated by the mini distribution, we have searched for alternative ways of solving for quantal parameters. We have derived a relationship between the expected variance in stimulus-evoked current amplitude and N, p, and the fractional contribution of intrinsic variance in mini amplitude to total variance in mini amplitude, W. This relationship allows us to determine the amount of error in calculated values for N and p that could be due to errors in guessing a value for W. We find that the values of N and p as determined by this relationship are relatively insensitive to the value of W. Taking the data from Borges et al. (1995), in which W is assumed to be 1, we find that the N and p values determined in that work are in error by no more than 20% in the absence of any constraint on the value of W. This implies that the probability of release in these cells during the depolarization protocol used is high, and the number of release sites in these cells is low.

Our results suggest that the errors that ambiguity in the value of W causes in estimating N and p using our equations is low. Of course, if an independent estimate of N, p, or W is available, the other parameters could all be determined unambiguously. We point out that in some cases an independent estimate of N is a reasonable approach to solving the other parameters. Some experiments have used antibody staining (Bekkers et al., 1990) or fluorescent dyes (Liu and Tsien, 1995) to localize single synaptic boutons, and in at least some cases a single bouton appears to represent a single release site (Liu and Tsien, 1995). By counting the number of boutons, then, one might get an estimate of N that is independent of quantal analysis in those systems, and solving for p and W using the means and variances of minis and stimulus-evoked synaptic currents then might be a reasonable approach.

The equations derived here are similar to those used previously to determine the locus of long-term potentiation without resorting to quantal analysis by detecting changes in the CV of evoked responses squared (Malinow and Tsien, 1990; Bekkers and Stevens, 1990). The CV^2 approach has some major limitations, as outlined in Faber and Korn (1991), two of which are also limitations for our equations. First, our equations assume that only a single presynaptic input is activated; activation of multiple inputs would render data uninterpretable by our methods because each input would have its own N, p, and A values, causing the distribution of evoked responses to be the sum of multiple binomials, each with a different quantal unit. Second, we have assumed that the probability of release is uniform at all sites. It is clear that in at least some systems, this assumption does not hold (Rosenmund et al., 1993; Hessler et al., 1993) and under these circumstances, Eq. 12 must be used to describe the variance in evoked release. This equation requires knowledge of the variance in probability of release at different sites. This variability can, in principle, be estimated at glutamatergic synapses using the NMDA receptor open channel blocker MK-801 without resorting to quantal analysis (Rosenmund et al., 1993; Hessler et al., 1993; Manabe and Nicoll, 1994; Huang and Stevens, 1995). It should be noted that, assuming a continuous distribution of probabilities of release (Huang and Stevens, 1995; see Manabe and Nicoll, 1994), the maximum value for σ^2_p is around 0.1 (assuming a flat distribution of p_x ranging in amplitude from 0 to 1), a value that could be used in Eq. 12 as a "worst-case" scenario. Finally, as has been discussed at length above, a limitation of this approach which should be emphasized is that these equations require the mini distribution measured to be identical to the distribution of uniquantal events from the same sites that generate multiquantal evoked release.

We thank David Attwell for comments on the manuscript, and Michael Turelli for useful suggestions and discussion.

This work was supported by NEI, EY04112 (MW) and a NSF predoctoral fellowship (MF).

REFERENCES

Bekkers, J.M. 1995. Synchronous and 9 synchronous EPSCs evoked in hippocampal slices: a test of the quantal model of neurotransmission. *Soc. Neurosci. Abstr.* 21:1091.

Bekkers, J. M., G. B. Richerson, and C. F. Stevens. 1990. Origin of variability in quantal size in cultured hippocampal neurons and hippocampal slices. *Proc. Natl. Acad. Sci. USA.* 87:5359–5362.

Bekkers, J. M., and C. F. Stevens. 1989. NMDA and non-NMDA receptors are co-localized at individual excitatory synapses in cultured rat hippocampus. *Nature.* 341:230–233.

Bekkers, J. M., and C. F. Stevens. 1990. Presynaptic mechanism for long-term potentiation in the hippocampus. *Nature.* 346:724–729.

Bekkers, J. M., and C. F. Stevens. 1991. Excitatory and inhibitory autaptic currents in isolated hippocampal neurons maintained in cell culture. *Proc. Natl. Acad. Sci. USA.* 88:7834–7838.

Bekkers, J. M., and C. F. Stevens. 1994. The nature of quantal transmission at central excitatory synapses. *In* Molecular and Cellular Mechanisms of Neurotransmitter Release. L. Stjärne, P. Greengard, S. Grillner, T. Hökfelt, and D. Ottoson, editors. Raven Press, New York. 261–273.

Bekkers, J. M., and C. F. Stevens. 1995. Quantal analysis of EPSCs recorded from small numbers of synapses in hippocampal cultures. *J. Neurophysiol.* 73:1145–1156.

Borges, S., E. Gleason, M. Turelli, and M. Wilson. 1995. The kinetics of quantal transmitter release from retinal amacrine cells. *Proc. Natl. Acad. Sci. USA.* 92:6896–6900.

Boyd, I. A., and A. R. Martin. 1956a. Spontaneous subthreshold activity at mammalian neuromuscular junction. *J. Physiol.* 132:61–73.

Boyd, I. A., and A. R. Martin. 1956b. The end plate potential in mammalian muscle. *J. Physiol.* 132:74–91.

De Koninck, Y., and I. Mody. 1994. Noise analysis of miniature IPSCs in adult rat brain slices: properties and modulation of synaptic $GABA_A$ receptor channels. *J. Neurophysiol.* 71:1318–1335.

del Castillo, J., and B. Katz. 1954. Quantal components of the end-plate potential. *J. Physiol.* 124:560–573.

Edwards, F. A. 1995. LTP—a structural model to explain the inconsistencies. *Trends Neurosci.* 18:250–255

Edwards, F. A., A. Konnerth, and B. Sakmann. 1990. Quantal analysis of inhibitory synaptic transmission in the dentate gyrus of rat hippocampal slices: a patch-clamp study. *J. Physiol.* 430:213–249.

Faber, D. S., and H. Korn. 1991. Applicability of the coefficient of variation method for analyzing synaptic plasticity. *Biophys. J.* 60: 1288–1294.

Faber, D. S., W. S. Young, P. Legendre, and H. Korn. 1992. Intrinsic quantal variability due to stochastic properties of receptor-transmitter interactions. *Science.* 258:1494–1498.

Fatt, P., and B. Katz. 1952. Spontaneous subthreshold activity at motor nerve endings. *J. Physiol.* 117:109–128.

Frerking, M., S. Borges, and M. Wilson. 1995. Variation in GABA mini-amplitude is the consequence of variation in transmitter concentration. *Neuron.* 15:885–895.

Hessler, N. A., A. M. Shirke, and R. Malinow. 1993. The probability of transmitter release at a mammalian central synapse. *Nature.* 366: 569–572.

Huang, E.P., and C.F. Stevens. 1995. Transmitter release probability function: a continuous distribution. *Soc. Neurosci. Abstr.* 21:1090.

Isaacson, J. S., and B. Walmsley. 1995. Counting quanta: direct measurements of transmitter release at a central synapse. *Neuron.* 15:875–884.

Jack, J. J. B., A. U. Larkman, G. Major, and K. J. Stratford. 1994. Quantal analysis of the synaptic excitation of CA1 hippocampal pyramidal cells. *In* Molecular and Cellular Mechanisms of Neurotransmitter Release. L. Stjärne, P. Greengard, S. Grillner, T. Hökfelt, and D. Ottoson, editors. Raven Press, New York. 275–299.

Jack, J. J. B., S. J. Redman, and K. Wong. 1981. The components of synaptic potentials evoked in cat spinal motoneurones by impulses in single group Ia afferents. *J. Physiol.* 321:65–96.

Jonas, P., G. Major, and B. Sakmann. 1993. Quantal components of unitary EPSCs at the mossy fibre synapse on CA3 pyramidal cells of rat hippocampus. *J. Physiol.* 472:615–663.

Korn, H., F. Bausela, S. Charpier, and D. S. Faber. 1993. Synaptic noise and multiquantal release at dendritic synapses. *J. Neurophysiol.* 70: 1249–1254.

Korn, H., and D. S. Faber. 1991. Quantal analysis and synaptic efficacy in the CNS. *Trends Neurosci.* 14:439–445.

Korn, H., A. Mallet, A. Triller, and D. S. Faber. 1982. Transmission at a central inhibitory synapse. II. Quantal description of release, with a physical correlate for binomial *n*. *J. Neurophysiol.* 48:679–707.

Korn, H., C. Sur, S. Charpier, P. Legendre, and D. S. Faber. 1994. The one-vesicle hypothesis and multivesicular release. *In* Molecular and Cellular Mechanisms of Neurotransmitter Release. L. Stjärne, P. Greengard, S. Grillner, T. Hökfelt, and D. Ottoson, editors. Raven Press, New York. 301–322.

Korn, H., A. Triller, A. Mallet, and D. S. Faber. 1981. Fluctuating responses at a central synapse: *n* of binomial fit predicts number of stained presynaptic boutons. *Science.* 213:898–901.

Kullmann, D. M. 1992. Quantal analysis using maximum entropy noise deconvolution. *J. Neurosci. Methods.* 44:47–57.

Kullmann, D. M. 1993. Quantal variability of excitatory transmission in the hippocampus: implications for the opening probability of fast glutamate-gated channels. *Proc. R. Soc. Lond. B.* 253:107–116.

Kullmann, D. M. 1994. Amplitude fluctuations of dual-component EPSCs in hippocampal pyramidal cells: implications for long-term potentiation. *Neuron.* 12:1111–1120.

Kullmann, D. M., and R. A. Nicoll. 1992. Long-term potentiation is associated with increases in quantal content and quantal amplitude. *Nature.* 357:240–244.

Lapin, L. 1975. Statistics: Meaning and Method. Harcourt Brace Jovanovich, New York.

Larkman, A., T. Hannay, K. Stratford, and J. Jack. 1992. Presynaptic release probability influences the locus of long-term potentiation. *Nature.* 360:70–73.

Larkman, A., K. Stratford, and J. Jack. 1991. Quantal analysis of excitatory synaptic action and depression in hippocampal slices. *Nature.* 350: 344–347.

Liley, A. W. 1956. The quantal components of the mammalian end-plate potential. *J. Physiol.* 133:571–587.

Liu, G., and R. W. Tsien. 1995. Properties of synaptic transmission at single hippocampal synaptic boutons. *Nature.* 375:404–408.

Malgaroli, A., and R. Tsien. 1992. Glutamate-induced long-term potentiation of the frequency of miniature synaptic currents in cultured hippocampal neurons. *Nature.* 357:134–139.

Malinow, R., and R. Tsien. 1990. Presynaptic enhancement shown by whole-cell recordings of long-term potentiation in hippocampal slices. *Nature.* 346:177–180.

Manabe, T., and R. Nicoll. 1994. Long-term potentiation: evidence against an increase in transmitter release probability in the CA1 region of the hippocampus. *Science.* 265:1888–1892.

Manabe, T., P. Renner, and R. Nicoll. 1992. Postsynaptic contribution to long-term potentiation revealed by the analysis of miniature synaptic currents. *Nature.* 355:50–55.

Murphy, T., J. Baraban, and W. Wier. 1995. Mapping miniature synaptic currents to single synapses using calcium imaging reveals heterogeneity in postsynaptic output. *Neuron.* 15:159–168.

Oliet, S., R. Malenka, and R. Nicoll. 1996. Bidirectional control of quantal size by synaptic activity in the hippocampus. *Science.* 271:1294–1297.

Otis, T., and I. Mody. 1992. Modulation of decay kinetics and frequency of GABAA receptor-mediated spontaneous inhibitory postsynaptic currents in hippocampal neurons. *Neuroscience.* 49:13–32.

Redman, S., and B. Walmsley. 1983. Amplitude fluctuations in synaptic potentials evoked in cat spinal motoneurones at identified group Ia synapses. *J. Physiol.* 343:135–145.

Rekling, J. 1993. Effects of met-enkephalin on GABAergic spontaneous miniature IPSPs in organotypic slice cultures of the rat hippocampus. *J. Neurosci.* 13:1954–1964.

Ropert, N., R. Miles, and H. Korn. 1990. Characteristics of miniature inhibitory postsynaptic currents in CA1 pyramidal neurones of rat hippocampus. *J. Physiol.* 428:707–722.

Rosenmund, C., J. D. Clements, and G. L. Westbrook. 1993. Nonuniform probability of glutamate release at a hippocampal synapse. *Science.* 262:754–757.

Silver, R., S. Traynelis, and S. Cull-Candy. 1992. Rapid-time course miniature and evoked excitatory currents at cerebellar synapses in situ. *Nature.* 355:163–166.

Sorra, K., and K. Harris. 1993. Occurrence and three-dimensional structure of multiple synapses between individual radiatum axons and their target pyramidal cells in hippocampal area CA1. *J. Neurosci.* 13:3736–3748.

Stricker, C., A. C. Field, and S. Redman. 1994. Probabilistic secretion of quanta at excitatory synapses on CA1 pyramidal neurons. *In* Molecular and Cellular Mechanisms of Neurotransmitter Release. L. Stjärne, P. Greengard, S. Grillner, T. Hökfelt, and D. Ottoson, editors. Raven Press, New York. 323–340.

Tang, C.-M., M. Margulis, Q.-Y. Shi, and A. Fielding. 1994. Saturation of postsynaptic glutamate receptors after quantal release of transmitter. *Neuron.* 13:1385–1393.

Tong, G., and C. Jahr. 1994. Block of glutamate transporters potentiates postsynaptic excitation. *Neuron.* 13:1195–1203.

Ulrich, D., and H.-R. Lüscher. 1993. Miniature excitatory synaptic currents corrected for dendritic cable properties reveal quantal size and variance. *J. Neurophysiol.* 69:1769–1773.

von Kitzing, E., P. Jonas, and B. Sakmann. 1994. Quantal analysis of excitatory postsynaptic currents at the hippocampal mossy fiber-CA3 pyramidal cell synapse. *In* Molecular and Cellular Mechanisms of Neurotransmitter Release. L. Stjärne, P. Greengard, S. Grillner, T. Hökfelt, and D. Ottoson, editors. Raven Press, New York. 235–260.

Walmsley, B., F. R. Edwards, and D. J. Tracey. 1988. Nonuniform release probabilities underlie quantal synaptic transmission at a mammalian excitatory central synapse. *J. Neurophysiol.* 60:889–908.

Wyllie, D., T. Manabe, and R. Nicoll. 1994. A rise in postsynaptic Ca^{2+} potentiates miniature excitatory postsynaptic currents and AMPA responses in hippocampal neurons. *Neuron.* 12:127–138.